RESEARCH ARTICLE
SOLID EARTH: GEOELECTROMAGNETICS

Earth and Planetary Physics
3: 435–443, 2019
doi: 10.26464/epp2019043

Characteristics of the coseismic geomagnetic disturbances recorded during the 2008 M_w 7.9 Wenchuan Earthquake and two unexplained problems

YaLi Wang[1*], Tao Xie[1], YanRu An[1,2], Chong Yue[1], JiuYang Wang[3], Chen Yu[1], Li Yao[1], and Jun Lu[1]

[1]China Earthquake Networks Center, Beijing 100045, China;

[2]Institute of Geophysics, China Earthquake Administration, Beijing 100081, China;

[3]Earthquake Observatory of Dalian, Liaoning Province, Dalian 116012, China

Abstract: Twenty-seven FHDZ-M15 combined geomagnetic observation systems (each of which is equipped with a fluxgate magnetometer and a proton magnetometer) had been installed in the China geomagnetic network before the 2008 Wenchuan earthquake, during which coseismic disturbances were recorded by 26 fluxgate magnetometer observatories. The geomagnetic disturbances have similar spatial and temporal patterns to seismic waves, except for various delays. Six proton magnetometer observatories recorded coseismic disturbances with very small amplitudes. In addition, fluxgate magnetometers registered large-amplitude disturbances that are likely to have included responses to seismic waves. However, two problems remain unresolved. First, why do these geomagnetic disturbances always arrive later than P waves? Second, why do the geomagnetic disturbances have spatial and temporal directivity similar to the main rupture direction of the earthquake? Solving these two problems may be crucial to find the mechanism responsible for generating these geomagnetic anomalies.

Keywords: Wenchuan Earthquake; co-seismic disturbance; geomagnetic field; fluxgate magnetometer; proton magnetometer

Citation: Wang, Y. L., Xie, T., An, Y. R., Yue, C., Wang, J. Y., Yu, C., Yao, L., and Lu, J. (2019). Characteristics of the coseismic geomagnetic disturbances recorded during the 2008 M_w 7.9 Wenchuan Earthquake and two unexplained problems. *Earth Planet. Phys.*, *3*(5), 435–443. http://doi.org/10.26464/epp2019043

1. Introduction

To date, considerable research on seismomagnetism has focused on extraction of earthquake precursor information. However, the correlations between precursor anomalies and earthquakes are often questioned. Coseismic electromagnetic signals have clear relationships with earthquake events and are easily extracted. Such signals have thus been identified as an effective means by which to study seismic transmission mechanisms, seismic energy conversion, and characteristics of near-surface media (Tang J et al., 2008, 2010). The study of coseismic electromagnetism promises not only to provide a reference for solving controversial problems in the current study of seismomagnetism but can also help to deepen our understanding of the physical processes of earthquakes from the perspective of electromagnetism (Huang QH, 2004; Iyemori et al., 1996).

In 1964, signals similar to seismic waves were recorded by magnetometers during the Alaskan earthquake. Some scientists attribute these signals to electromagnetic vibrations caused by earthquakes; others believe that they represent the vibration of a magnetic instrument (Eleman, 1966). Some indications of coseismic magnetic pulses have been found in Kamchatka ULF observations (Molchanov et al., 2002); Nagao et al. (2000) found that the duration of a coseismic electric pulse sometimes exceeds the length of the corresponding seismic pulse. They interpreted this in terms of an electrokinetic phenomenon, but this observation could also be explained by a seismoinductive effect (Nagao et al., 2000). Scientists have employed theoretical analyses and numerical calculations in pursuit of the mechanism responsible for generating coseismic geomagnetic signals (Huang QH and Sobolev, 2002; Ren HX et al., 2010a, b). In recent years, many studies have sought to explain the mechanism of seismic geomagnetism by examining electrokinetic effects (Ren HX et al., 2012; Gao YX et al., 2014), motional induction effects (Okubo et al., 2011), coupling relationships between the geomagnetic field and the spatial ionosphere (Zhao BQ and Hao YQ, 2015), etc.

The Wenchuan earthquake, which occurred in China at 06:28:04 (UT) on May 12, 2008, was a very strong and disastrous shallow earthquake. Zhao BQ and Hao YQ (2015) reported that the Wenchuan earthquake induced local magnetic disturbances at a minimum of three observatories, namely, COQ, ENS, and GYX, and that the maximum peak-to-peak amplitude of the residual *D* component was approximately 1′ (Zhao BQ and Hao YQ, 2015). Tang J et al. (2008) found that when aftershocks occurred following the Wenchuan earthquake, coseismic signals appeared in almost all

Correspondence to: Y. L. Wang, wang_violin@163.com
Received 15 APR 2019; Accepted 28 JUN 2019.
Accepted article online 05 AUG 2019.

the components of the electric and magnetic fields (Tang J et al., 2010).

However, most of these studies have been limited to analysis of data from individual observatories; few studies have been conducted on the temporal and spatial characteristics of the coseismic geomagnetic disturbances generated by the Wenchuan earthquake. At present, coseismic geomagnetic anomalies are not sufficiently understood, and the mechanism responsible for the formation of geomagnetic anomalies is still unclear.

2. Data Source

Simultaneous observations of seismic and electromagnetic phenomena at the same place give us a unique opportunity to study the correlation between the temporal variations of local seismicity and the parameters of the electromagnetic field (Gladychev et al., 2002). Before the M_w 7.9 earthquake struck Wenchuan in 2008, a geomagnetic network of more than 100 observatories had been established across mainland China. Among these observatories, 27 were equipped with an FHDZ-M15 combined geomagnetic observation system, consisting of a FGE fluxgate magnetometer and a GSM-19F OVERHAUSER proton precession magnetometer. The resolution of these FHDZ-M15 observation system is 0.1 nT, their band pass is DC–0.3 Hz, and the sampling rate is 1 Hz. The resolution of the GSM-19F OVERHAUSER magnetometer can reach 0.01 nT, and its maximum sampling interval is 0.2 s. The FGE magnetometers recorded the *H, D*, and *Z* components of the geomagnetic field, and the GSM-19F OVERHAUSER proton precession magnetometers recorded the *F* component. The time at each FHDZ-M15 observation system was provided automatically by a GPS device, with temporal accuracy better than 1 ms/d. Due to the good stability and high sensitivity of these FHDZ-M15 observation systems, in this paper we use the data they collected during the Wenchuan earthquake to study the temporal and spatial characteristics of that event's coseismic geomagnetic disturbances.

Proton magnetometers utilize a hydrogen-containing liquid to excite free electrons and use the coupling effect of these electrons on protons to induce proton magnetization and generate Larmor precession motion around the magnetic field. The magnetic field can then be measured through the precession frequency of the proton.

The principle of a fluxgate magnetometer is based on the nonlinear magnetization of magnetic core materials. The nonlinear magnetization of soft magnetic materials in an ambient magnetic field is used because of their high permeability and easy saturation. Under the magnetization induced by alternating exciting signals, the magnetic properties of the magnetic core will change periodically from saturated to unsaturated. As a result, an induction coil wound around the magnetic core will produce a modulation signal proportional to the external magnetic field; a description of the field can be extracted from this signal by means of a special device (Piil-Henriksen et al., 1996).

Twenty observatories were equipped with both an FHDZ-M15 geomagnetic observation system and a strong motion seismograph. Figure 1 shows the locations of the magnetometers and seismographs. For most of the observatories, including CD2, TOH, TCH, HAZ, HTB, LZH, and MZL, the magnetometer and seismograph were deployed at the same site, and the distance between them was less than 2 km. At some observatories, the two instruments were further from each other. At GYA, for example, the linear distance between the two instruments was 25 km, and the difference in their distances from the event epicenter was 11 km. At LSA and DL2, the linear distance between the magnetometer and seismograph was 20 km. We were unable to acquire strong motion data from 7 observatories, namely, KSH, GOM, SHY, JFE, JHA, SGA, and SQH.

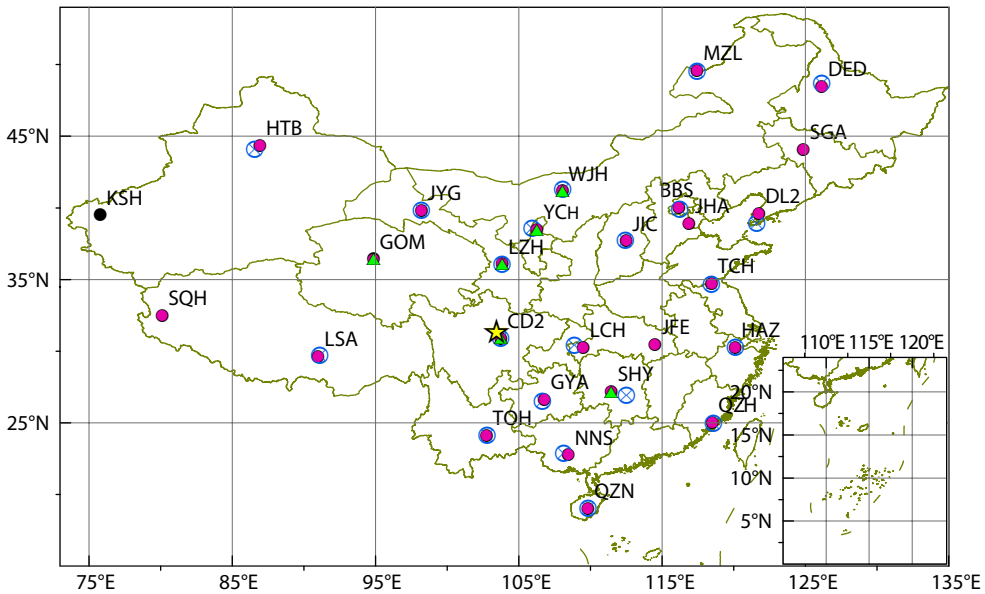

Figure 1. Distribution of geomagnetic observatories and seismographs. The dots represent FHDZ-M15 geomagnetic observation systems; red dots denote those with fluxgate coseismic detectors, green triangles denote those with proton probe detectors. The blue circles with crosses indicate locations of seismographs. The yellow star marks the epicenter of the Wenchuan earthquake.

3. Coseismic Geomagnetic Disturbances and Analysis

We examined all the data recorded on May 12, 2008, from the 27 observatories with an FHDZ-M15 observation system. The coseismic disturbances were observed by both fluxgate and proton probes. However, the disturbances observed by the two probes were very different.

3.1 Coseismic Disturbances Observed by Fluxgate Magnetometers

Coseismic disturbances similar to seismic waveforms were found in the *H*, *D*, and *Z* components at 26 observatories but were not observed at KSH.

Similar to seismic waves, geomagnetic disturbances (hereafter denoted as M waves) also have two types of waveform components. One component is similar to a P wave, which arrives first and has a smaller amplitude; the other is similar to an S wave, which has a larger amplitude but arrives later (see Figure 2). These two waves almost overlapped at CD2 due to the proximity of this observatory to the epicenter. However, these two waves were distinctly separated at DED, which is 2740 km away from the epicenter.

We selected the waveform data from the seismograph closest to a magnetometer observation point and picked the arrival times of the seismic P waves; the results are shown in Figure 2. To our surprise, the disturbance from the geomagnetic field was not synchronous with the P wave arrival time. At CD2, which is the closest observatory to the epicenter at 34 km, the coseismic geomagnetic disturbance occurred at 06:28:17 (UT), while the P wave arrived at 06:28:06. At the farthest observatory, DED, the onset time of the geomagnetic disturbance was 06:33:26, and the strong seismograph recorded the P wave arrival time at 06:33:21. Regardless of the arrival time difference between the P wave and the M wave, the M wave always lagged behind the P wave.

Figure 3 depicts the relationship among the M-wave arrival time, P-wave arrival time, and epicentral distance. Contrasting colors are used in this figure to distinguish different observatories. Here, to avoid redundancy, we show only the abnormal changes in the *D* components at each observatory; the *H* and *Z* components have similar variations.

As we expected, there is a generally linear relationship between P wave arrival time and epicentral distance; i.e., the closer the strong motion observatory is to the epicenter, the earlier the seismic P wave arrives, and the farther the observatory is from the epicenter, the later the P wave arrives (see the magenta travel-time curve in Figure 3).

The spatial distribution of arrival time of M waves (i.e., geomagnetic disturbance) also roughly, but not exactly, conforms to that of P waves (see the black fitting curve in Figure 3). The M wave is more complicated than a seismic wave. At some observatories, such as CD2 and HAZ, the arrival times of the P wave and M wave were not very different. At other observatories, the M wave lagged significantly behind the P wave. At HTB, which recorded the longest lag, the straight-line distance between the ground motion and geomagnetic instruments was less than 200 m. Yet at HTB the P wave arrived at 06:32:21, 403 s before the M wave (at 06:39:04).

3.2 Coseismic Disturbances Recorded by Proton Magnetometers

In contrast, the *F*-component disturbances recorded by the OVERHAUSER proton magnetometers were not significant. For example, the amplitude of variation in the *F* component at CD2 was only 16.11 nT, which is negligible compared to the changes in the *H* and *Z* components, which reached as high as 1000+ nT (Figure 2a). Of the 26 geomagnetic observatories that recorded a disturbance, only six observatories—namely, CD2, YCH, SHY, YCH, GOM, and WJH (Table 1)—recorded minor abnormal coseismic changes in the *F* component. Among the 6 above-mentioned observatories, the geomagnetic changes recorded by CD2, GOM, and SHY were pulse signals, while those recorded by LZH, YCH, and WJH were continuous high-frequency signals (Figure 4). A very small pulse was recorded at 06:28:13 (9 s after the Wenchuan earthquake) by CD2, while a very large pulse was recorded 21 s later (at 06:28:34). Then, 389 s after the Wenchuan earthquake struck, a pulse was recorded by SHY at 06:34:33. At GOM, a short pulse was observed at 06:33:32 (328 s after the Wenchuan earthquake). The continuous high-frequency signals recorded by LZH, YCH, and WJH began at 06:31:18, 06:32:53, and 06:34:03, respectively. In ad-

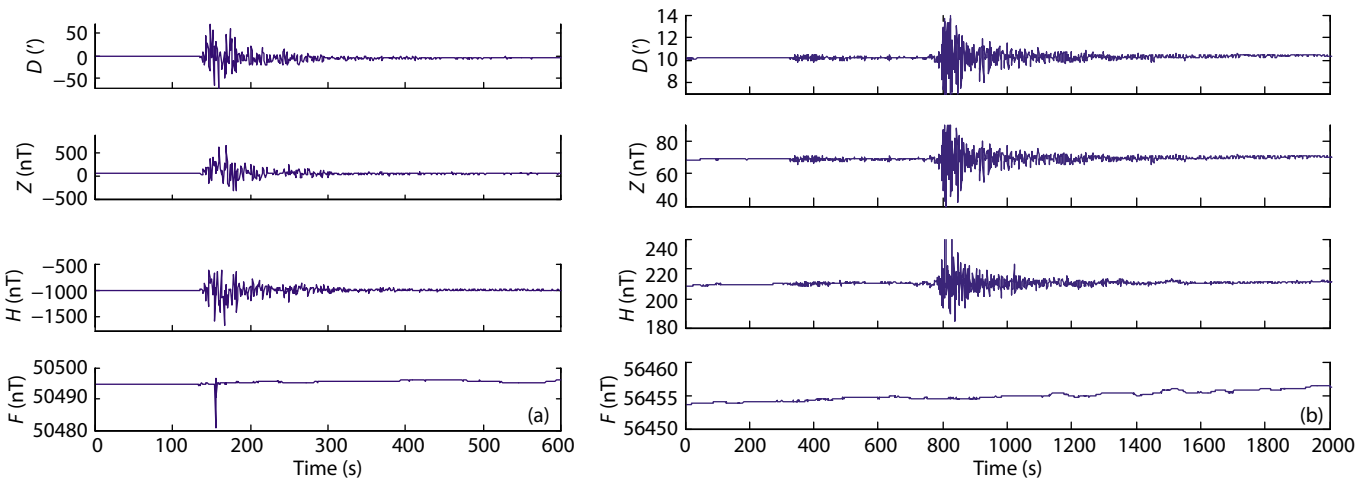

Figure 2. Coseismic geomagnetic anomaly curves from the CD2 (a) and DED observatories (b).

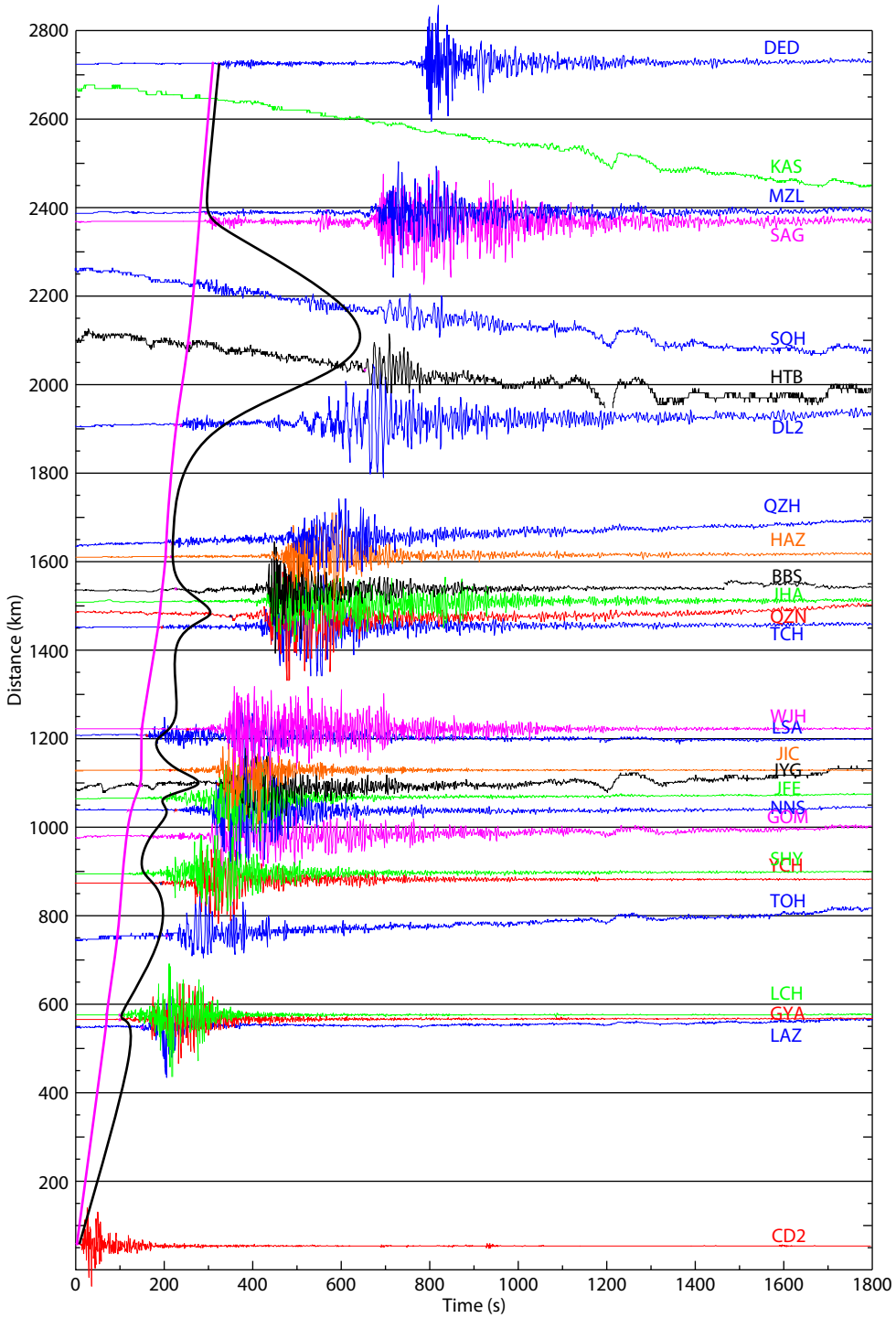

Figure 3. Coseismic disturbances in the *D* components recorded by 27 fluxgate probes, plotted against their distances from the epicenter. The horizontal axis is time, and the vertical axis is epicentral distance. The origin of the horizontal axis represents the time of the earthquake, i.e., 06:28:04 (UT). The travel time curves show first arrival of P waves (magenta) recorded by seismographs and the fit curve (black) of the magnetic disturbances onset times (to highlight the arrival time, different scales are used for each observatory, so the amplitudes are not comparable.)

dition, the coseismic signals recorded by the proton magnetometers always arrived later than the similar S-wave signals recorded by the fluxgate magnetometers.

3.3 Comparison and Analysis

Table 1 shows that the coseismic geomagnetic disturbances observed by the proton magnetometer probes were much smaller than those observed by the fluxgate probes. It seems that the proton magnetometer probes recorded only pulse signals and some high-frequency disturbances; no waveforms similar to seismic waves were recorded. The farthest observatory that recorded an *F*-component disturbance is WJH, which is 2370 km from the epicenter. The proton magnetometers that detected coseismic an-

Table 1. Seismic P wave and geomagnetic disturbances

Station	Epicentral distance (km)	First arrivalof P wave (hh:mm:ss)	Time of M wave (hh:mm:ss)	Time difference of M and P wave (s)	Amplitude of geomagnetic disturbance			
					D (′)	*H* (nT)	*Z* (nT)	*F* (nT)
CD2	34	06:28:06	06:28:17	11	154.75	1044.86	983.76	16.11
LZH	565	06:29:19	06:30:33	74	2.59	8.32	9.22	0.32
GYA	597	06:29:21	06:29:32	11	13.03	87.7	89.56	–
LCH	644	06:29:13	06:29:47	34	40.24	239.33	317.49	–
TOH	769	06:29:41	06:31:31	110	0.37	0.63	0.97	–
YCH	875	06:29:58	06:31:21	83	113.96	993.2	665.46	0.87
SHY*	995		06:30:06		7.04	91.32	103.9	3.68
GOM*	995		06:31:58		1.19	0.97	0.52	0.2
NNS	1017	06:30:13	06:32:07	114	4.59	30.97	42.42	–
JFE*	1060		06:33:32		5.29	73.92	66.50	–
JYG	1086	06:30:26	06:33:34	188	0.73	0.89	0.63	–
JIC	1113	06:30:25	06:31:49	84	81.85	655.16	403.16	–
WJH	1218	06:30:38	06:31:57	79	53.84	372.63	241.98	0.85
LSA	1188	06:30:35	06:30:42	7	3.17	7.04	7.3	–
TCH	1462	06:31:07	06:31:13	6	6.57	54.33	49.28	–
QZN	1480	06:31:08	06:34:00	172	1.49	12.17	25.36	–
JHA*	1506		06:34:54		6.43	14.29	9.79	–
BBS	1523	06:31:16	06:31:20	4	7.66	110.52	62.91	–
HAZ	1598	06:31:26	06:31:28	2	6.31	73.73	82.81	–
QZH	1633	06:31:27	06:31:35	8	1.16	0.77	0.44	–
DL2	1872	06:31:59	06:32:01	2.5	2.42	21.38	13.76	–
HTB	2070	06:32:21	06:39:04	403	0.36	1.07	0.57	–
SQH*	2206		06:39:26		0.17	–	–	–
SGA*	2372		06:32:58		4.48	42.95	30.16	–
MZL	2374	06:32:48	06:33:00	12	6.31	36.35	13.99	–
KSH	2666				–	–	–	–
DED	2740	06:33:21	06:33:26	5	8.67	63.68	24.58	–

Note: * indicates we do not have seismic data from these observatories; '–' means no apparent disturbance was detected.

omalies cover a large area, although it is smaller than the area in which anomalies were observed by the fluxgate probes. The largest coseismic changes detected by both types of probe were to the northeast.

For the fluxgate probes, the amplitudes of the anomalies in the *H* and *Z* components at a given observatory were on the same order. However, the anomaly amplitudes at different observatories were very different. The amplitudes of the anomalies decreased with increasing epicentral distance, and the amplitude of the disturbance at most of observatories reached hundreds of nT. The geomagnetic disturbance at CD2, which is the closest observatory to the epicenter, was the largest at 1000^{+} nT. In contrast, only a few nT of variation was recorded at HTB, which is 2374 km from the epicenter. We also found that the amplitude at the farthest observatory was not the smallest. Although DED is the farthest from the epicenter, the magnitude of the anomaly at DED was much larger than those at TOH and SQH, which are much closer.

The attenuation of the abnormal amplitude varied in different directions. There was no obvious coseismic response at KSH, located 2666 km northwest of the epicenter, but the abnormality detected at the DED, 2740 km to the northeast of the epicenter, was still very significant (Figure 5).

For the fluxgate probes, the coseismic signals to the northeast were smaller, and they also attenuated much more slowly (Figure 5). For the proton probes, although coseismic changes were observed at only six observatories, these observatories were clustered primarily to the northeast and northwest (Figure 1).

4. Discussion

Of the 27 observatories with fluxgate probes, obvious magnetic disturbances were recorded at 26 of them. The only exception

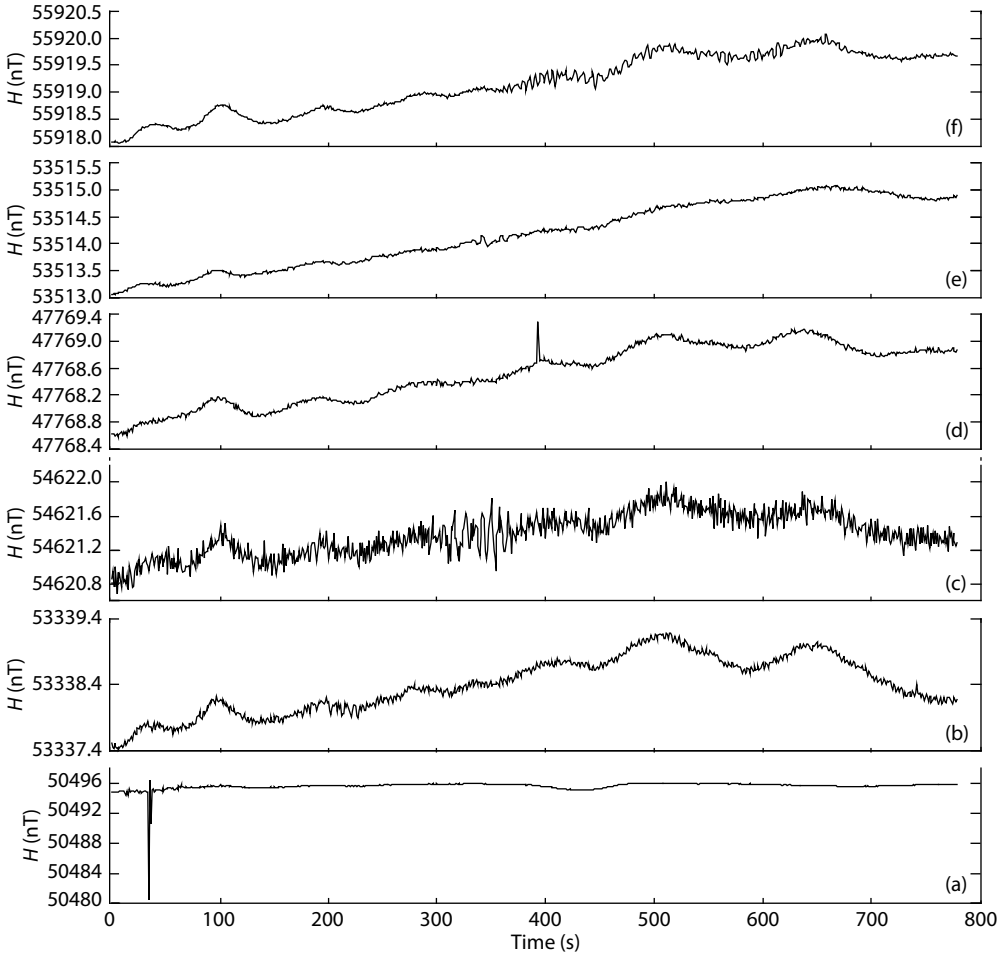

Figure 4. Coseismic Geomagnetic disturbances recorded by proton probes at 6 observatories: (a) CD2; (b) LZH; (c) YCH; (d) SHY; (e) GOM; and (f) WJH.

was at KSH, which is 2666 km from the epicenter. The range of geomagnetic disturbances caused by the Wenchuan earthquake was very broad. Abnormal changes were observed from CD2, which is 34 km from the epicenter, to DED, which is 2729 km from the epicenter. The latter observatory is far beyond the 1000 km anomaly range proposed by Zhao (Zhao QB and Hao YQ, 2015).

We used the *Kp* indices from May 12, 2008 to evaluate the geomagnetic activity (Table 2). ΣKp denotes the sum of the 8 *Kp* indices for each day. Generally, if $\Sigma Kp > 30$, there is strong geomagnetic activity (Hattori et al., 2002). On the day of the Wenchuan earthquake, $\Sigma Kp = 6^-$, which means that the geomagnetic field was very inactive. The amplitudes of most of the coseismic disturbances recorded by fluxgate probes reached hundreds of nT. In contrast, the seasonal variation of the geomagnetic field is only a few nT (Nagao et al., 2003). The typical solar daily variation ranges from a few nT to tens of nT. Magnetic field changes can range from several tens to hundreds of nT when a magnetic storm occurs, and only the largest can produce variations exceeding 1000 nT (Xu WY, 2003). Geomagnetic activity was quiet on the day of the Wenchuan earthquake; thus, the disturbances recorded by the fluxgate magnetometers are unlikely to have originated from an external field.

Reid (1914) found that many of the coseismic geomagnetic signals observed before the early 1900s may have been generated by mechanical vibration of the sensor due to the arrival of seismic waves. Since the mid-1960s, with the use of proton magnetometers, these reported abnormal magnitudes have declined rapidly (Johnston et al., 1984; Park et al., 1993; Johnston, 1974; Reid, 1914). Some scientists attribute coseismic geomagnetic signals to the mechanical vibration of magnetometers (Eleman, 1966).

Depending on the working principle, the induction coil structure in some fluxgate magnetometers may lead to an additional induced electromotive force generated by mechanical vibration, resulting in disturbances on coseismic geomagnetic recordings. Therefore, this kind of fluxgate instrument can record not only the possible coseismic changes in the geomagnetic field but also the response of the magnetometer itself to the vibration process.

We tend to believe that the main component of the ultra-large-scale coseismic disturbances recorded by the fluxgate instruments represents the responses of the instruments themselves to vibration, while only a small part signifies the coseismic variation in the geomagnetic field. The latter, which was recorded by the proton precession magnetometers, is very small in comparison and cannot be easily distinguished.

The coseismic changes observed by the proton magnetometers

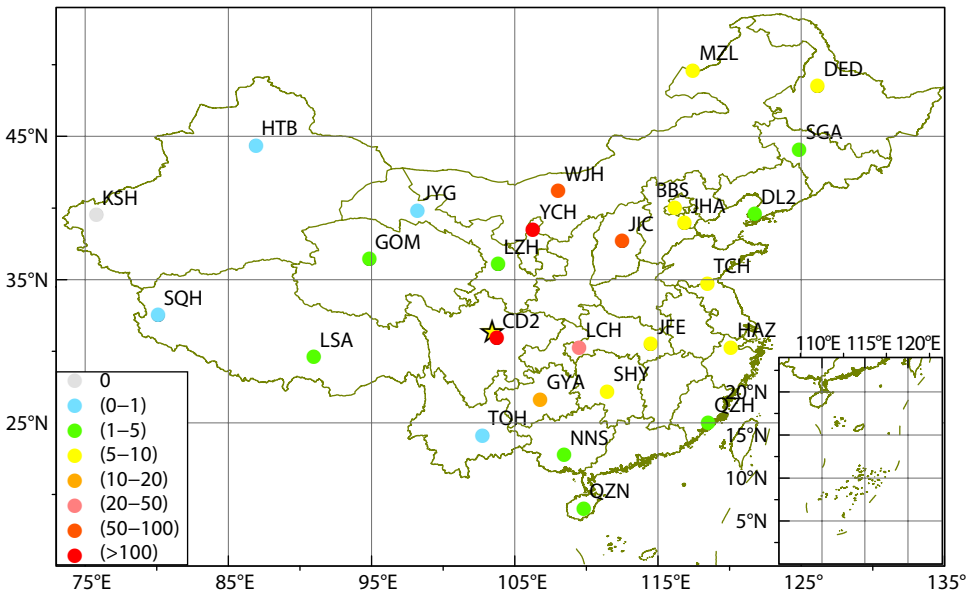

Figure 5. Spatial distribution of the *D*-component disturbance amplitude.

Table 2. *Kp* index on the day of the Wenchuan earthquake

Kp[8]								Sum
0^+	0^+	1^-	1^-	0^+	1	1	1^+	6^-

appeared after similar coseismic S-wave signal recorded by the fluxgate probe, and the abnormal changes in the geomagnetic field seemed to be related to the vibration amplitude.

However, there are still two unexplained problems. First, why did the geomagnetic disturbances always arrive later than the seismic waves? If the vibration of the instrument caused the abnormal change, theoretically the disturbances in the geomagnetic field should have arrived at the same time as the seismic waves. We found that for all observatories, the geomagnetic changes occurred more or less later than the arrivals of the seismic waves. We contacted the staff at more than 20 observatories, and they believed that the system times of the magnetometers were accurate because the instrument times were provided automatically by GPS devices.

In fact, there have been previous reports of geomagnetic anomalies that were not synchronous with the arrivals of seismic waves. Cha N et al. (2016) found that the seismic P wave arrived at the DL2 geomagnetic observatory at 06:32:10.00 (UT), and the S wave arrived at 06:35:57.6, while changes associated with geomagnetic abnormalities occurred from 06:37:54 to 06:51:40, i.e., 344 s later than the P-wave arrival and 116 s later than the S-wave arrival (Cha N et al., 2016). Changes in electromagnetic signals were recorded 3 s after the Izmit earthquake in 1999 (Honkura et al., 2002). Zhao BQ and Hao YQ (2015) similarly found that the geomagnetic disturbances recorded during the Wenchuan earthquake occurred after the arrival of seismic waves (see Fig. 6 and Fig. 7 of Zhao BQ and Hao YQ, 2015). Nevertheless, the phenomena mentioned in these reports, i.e., the asynchronicity of geomagnetic disturbances and seismic waves, have not been sufficiently studied.

Second, why did the geomagnetic disturbances have spatial and temporal directivity similar to the main rupture direction of the earthquake (see Figure 5)? Of all the 26 observatories that recorded abnormal changes, in addition to the very large anomaly at CD2, which is near the epicenter, the abnormal amplitudes at LCH, YCH, WJH and JIC to the northeast of the epicenter were also as high as several hundred nT, while those at JYG and HTB to the northwest and at SQH to the southwest were very small. The anomalies decayed slowly to the northeast. No abnormalities were detected at KSH to the northwest of the epicenter, while the disturbance at DED to the northeast had an amplitude of several tens of nT. Although SQH and SGA are almost the same distance from the epicenter, the geomagnetic disturbance at SQH appeared at 06:39:26, while the abnormal occurrence time at SGA was 06:32:58, a difference of 368 s. The geomagnetic disturbance time at MZL, which is also located to the northeast of the epicenter, was 06:33:00. Only 2 s separated the geomagnetic disturbances recorded at SGA and MZL. In addition, the time difference between the P waves and M waves also had a similar directivity. At observatories to the northeast of the epicenter, the M wave arrived very soon after the P wave, and the time difference between them was relatively small, while the same time difference at observatories to the northwest and southwest was relatively large.

If the disturbance recorded by a fluxgate instrument is caused by vibration, its directivity could be related to the propagation of vibration energy, but the directivity of the abnormal proton magnetometer observatory distribution cannot be explained by this theory. Further research is needed to determine whether this directivity is only a random phenomenon or whether there is a deeper mechanism behind it.

5. Conclusions

A wide range of geomagnetic disturbances was observed by both fluxgate and proton magnetometers during the Wenchuan earthquake. Anomalies recorded by fluxgate magnetometers have waveforms similar to seismic waves. The characteristics of the spatial and temporal attenuation of these anomalies are also similar to those of seismic waves. However, the geomagnetic disturbances are not exactly identical to seismic waves. These geomagnetic disturbances do not arrive at the same time as seismic waves but lag behind them.

Geomagnetic disturbances have obvious directivity with regard to their arrival time, timing differences with P waves, amplitude, and attenuation. Their directivity is similar to that of the main rupture of the Wenchuan earthquake. This shows that geomagnetic disturbance anomalies are related to the propagation of energy associated with the earthquake rupture.

We tend to believe that the main components of the disturbances in the fluxgate geomagnetic records acquired during the Wenchuan earthquake are seismograph effects. Only a small part of these disturbances represents the coseismic changes in the geomagnetic field, and this component is not easily distinguishable.

However, there are two problems for which mechanical vibrations cannot account. The first is that geomagnetic disturbances are not synchronous with seismic waves; the second is the relationship between the geomagnetic anomaly directivity and the main rupture direction. The answers to these two questions may be the keys to finding the mechanism responsible for generating these geomagnetic anomalies.

Acknowledgments

The National Key R & D Program of China (2017YFC1500502) provides the funding for this work. The Geomagnetic Network Center of China provided the geomagnetic data; the seismic waveform data were provided by the China Earthquake Network Center. The *Kp* indexes were obtained from WDC (http://wdc.kugi.kyoto-u.ac.jp/kp/index.html). We thank Dr. Yalu Ma and Dr. Li Sun for giving us great help with the seismic data. We are also grateful to Prof. Fu Zhang of Tonghai Earthquake Observatory and Prof. Xiaomei Wang of Institute of Geophysics, China Earthquake Administration, for useful discussions. We acknowledge the excellent review of two anonymous reviewers, which were of great help toward the improvement of our manuscript.

References

Cha, N., Sun, Y. M., Yin, Y. N., and Wang, X. R. (2016). The geomagnetic coseismic effect of strong earthquake of Dalian Geomagnetic station in Liaoning. *J. Dis. Prev. Reduct.* (*in Chinese*), *32*(2), 28–31. https://doi.org/10.13693/j.cnki.cn21-1573.2016.02.005

Eleman, F. (1966). The response of magnetic instruments to earthquake waves. *J. Geomag. Geoelectr.*, *18*(1), 43–72. https://doi.org/10.5636/jgg.18.43

Gao, Y., X., Chen, X. F., Hu, H. S., Wen, J., Tang, J., and Fang, G. Q. (2014). Induced electromagnetic field by seismic waves in Earth's magnetic field. *J. Geophys. Res.*: *Solid Earth*, *119*(7), 5651–5682. https://doi.org/10.1002/2014JB010962

Gladychev, V., Baransky, L., Schekotov, A., Fedorov, E., Pokhotelov, O., Andreevsky, S., Rozhnoi, A., Khabazin, Y., Belyaev, G., Noda, Y. (2002). Some preliminary results of seismo-electromagnetic research at Complex Geophysical Observatory, Kamchatka. In M. Hayakawa, et al. (Eds.), *Seismo Electromagnetics*: *Lithosphere-Atmosphere-Ionosphere Coupling* (pp. 421-432). Tokyo: TERRAPUB.

Honkura, Y., Matsushima, M., Oshiman, N., Tunçer, M. K., Bariş, Ş., Ito, A., Iio, Y., and Işikara, A. M. (2002). Small electric and magnetic signals observed before the arrival of seismic wave. *Earth, Planets Space*, *54*(12), e9–e12. https://doi.org/10.1186/BF03352449

Huang, Q. H., and Sobolev, G. A. (2002). Precursory seismicity changes associated with the Nemuro Peninsula earthquake, January 28, 2000. *J. Asian Earth Sci.*, *21*(2), 135–146. https://doi.org/10.1016/S1367-9120(02)00032-9

Huang, Q. H. (2004). Application of electromagnetism in earthquake research. *Oil Geophys. Prospect.* (*in Chinese*), *39*(S1), 75–79, 84. https://doi.org/10.13810/j.cnki.issn.1000-7210.2004.s1.018

Iyemori, T., Kamei, T., Tanaka, Y., Takeda, M., Hashimoto, T., Araki, T., and Oshiman, N. (1996). Co-seismic geomagnetic variations observed at the 1995 Hyogoken-Nanbu earthquake. *J. Geomag. Geoelectr.*, *48*(8), 1059–1070. https://doi.org/10.5636/jgg.48.1059

Johnston, M. J. S. (1974). Preliminary results from a search for regional tectonomagnetic effects in California and western Nevada. *Tectonophysics*, *23*(3), 267–275. https://doi.org/10.1016/0040-1951(74)90026-2

Johnston, M. J. S., Mueller, R. J., Ware, R. H., and Davis, P. M. (1984). Precision of geomagnetic field measurements in a tectonically active region. *J. Geomag. Geoelectr.*, *36*(13), 83–95. https://doi.org/10.5636/jgg.36.83

Molchanov, O., Kulchitsky, A., and Hayakawa, M. (2002). ULF emission due to inductive seismo-electromagnetic effect. In M. Hayakawa, et al. (Eds.), *Seismo Electromagnetics*: *Lithosphere-Atmosphere-Ionosphere Coupling* (pp. 153-162). Tokyo: TERRAPUB.

Nagao, H., Iyemori, T., Higuchi, T., and Araki, T. (2003). Lower mantle conductivity anomalies estimated from geomagnetic jerks. *J. Geophys. Res.*: *Solid Earth*, *108*(B5), 2254. https://doi.org/10.1029/2002JB001786

Nagao, T., Orihara, Y., Yamaguchi, T., Takahashi, I., Hattori, K., Noda, Y., Sayanagi, K., and Uyeda, S. (2000). Co-seismic geoelectric potential changes observed in Japan. *Geophys. Res. Lett.*, *27*(10), 1535–1538. https://doi.org/10.1029/1999GL005440

Okubo, K., Takeuchi, N., Utsugi, M., Yumoto, K., and Sasai, Y. (2011). Direct magnetic signals from earthquake rupturing: Iwate-Miyagi earthquake of M 7.2. *Japan. Earth Planet. Sci. Lett.*, *305*(1-2), 65–72. https://doi.org/10.1016/j.epsl.2011.02.042

Park, S., Johnston, M. J. S., Madden, T. R., Morgan, F. D., and Morrison, H. F. (1993). Electromagnetic precursors to earthquakes in the Ulf band: a review of observations and mechanisms. *Rev. Geophys.*, *31*(2), 117–132. https://doi.org/10.1029/93RG00820

Piil-Henriksen, J., Merayo, J. M. G., Nielsen, O. V., Petersen, H., Raagaard Petersen, J., and Primdahl, F. (1996). Digital detection and feedback fluxgate magnetometer. *Meas. Sci. Technol.*, *7*(6), 897–903. https://doi.org/10.1088/0957-0233/7/6/006

Reid, H. F. (1914). The free and forced vibrations of a suspended magnet: 1 Theory . *Terr. Atmos. Electr.*, *19*(2), 57–72. https://doi.org/10.1029/TE019i002p00057

Ren, H. X., Huang, Q. H., and Chen, X. F. (2010a). Analytical regularization of the high-frequency instability problem in numerical simulation of seismoelectric wave-fields in multi-layered porous media. *Chinese. J. Geophys.* (*in Chinese*), *53*(3), 506–511. https://doi.org/10.3969/j.issn.0001-5733.2010.03.004

Ren, H. X., Huang, Q. H., and Chen, X. F. (2010b). A new numerical technique for simulating the coupled seismic and electromagnetic waves in layered porous media. *Earthq. Sci.*, *23*(2), 167–176. https://doi.org/10.1007/s11589-009-0071-9

Ren, H. X., Chen, X. F., and Huang, Q. H. (2012). Numerical simulation of coseismic electromagnetic fields associated with seismic waves due to finite faulting in porous media. *Geophys. J. Int.*, *188*(3), 925–944. https://doi.org/10.1111/j.1365-246X.2011.05309.x

Tang, J., Zhan, Y., Wang, L. F., Xu, J. L., Zhao, G. Z., Chen, X. B., Dong, Z. Y., Xiao,

Q. B., Wang, J. J., … Xu, G. J. (2008). Coseismic signal associated with aftershock of the M_S 8.0 Wenchuan earthquake. *Seismol. Geol.* (*in Chinese*), *30*(3), 739–745. https://doi.org/10.3969/j.issn.0253-4967.2008.03.012

Tang, J., Zhan, Y., Wang, L. F., Dong, Z. Y., Zhao, G. Z., and Xu, J. L. (2010). Electromagnetic coseismic effect associated with aftershock of Wenchuan M_S8.0 earthquake. *Chinese J. Geophys.*, (*in Chinese*), *53*(3), 526–534. https://doi.org/10.3969/j.issn.0001-5733.2010.03.006

Xu, W. Y. (2003). *Geomagnetism* (pp. 221-287) (in Chinese). Beijing: Earthquake Publishing House.

Zhao, B. Q., and Hao, Y. Q. (2015). Ionospheric and geomagnetic disturbances caused by the 2008 Wenchuan earthquake: a revisit. *J. Geophys. Res.*: *Space Phys.*, *120*(7), 5758–5777. https://doi.org/10.1002/2015JA021035